

---

**References**

- Barnett, J. D., Bean, V. E., Hall, H. T., 1966, *J. Appl. Phys.*, **37**, 875.  
Epain, R., Susse, C., Vodar, B., 1967, *C. R. Acad. Sci., Ser. A*, **265**, 323-326.  
Hall, H. T., 1960, "High pressure methods" in *International Symposium on High Temperature Technology*, Stanford Research Institute, Ed. C. A. Scarlott (McGraw-Hill, New York).  
Kawai, N., Mochizuki, S., Fujita, H., 1971, *Phys. Lett. A*, **34**, (2), 107.  
Kumazawa, M., 1971, *High Temp. - High Pressures*, **3**, 243-260.
- 

## Pressure determination in a high-pressure cell for Raman spectroscopy at 4.2 K

D Fabre

Laboratoire des Interactions Moléculaires et des Hautes Pressions, CNRS, 92190 Meudon-Bellevue, France

When using Raman spectroscopy for investigating molecular interactions under pressure it is necessary to know the density or the pressure, neither of which can be readily determined in low-temperature experiments. The high-pressure Raman cell used here is of a piston-cylinder type (Jean-Louis and Vu, 1972) with four sapphire windows. It is not suited to density measurements, largely because of the presence of windows. Infrared absorption studies of hydrogen at 4.2 K have been made up to 14 kbar with such a device by Jean-Louis and Vu (1972) in which the pressure was determined from the pressure shift of the energy gap of GaSb immersed in the sample, but this method can be applied only in the infrared range.

The pressure in the sample cannot be estimated directly from the applied load, owing to the large friction in the apparatus, especially at low temperatures, although the friction can be taken into account by making several pressure runs (Bridgman, 1942; Steward, 1956); this provides a means of calibrating a sensor. First, we tried to detect the pressure in the cell by its effect on the Raman librational spectrum of the cell windows, but the sapphire scattering intensity is too weak to allow precise measurements. On the other hand, the window fluorescence, excited by the incident light scattered in the sample, has a fairly high intensity and its spectral pressure shift can be measured with precision; we used it as a pressure sensor. The method resembles that of Barnett *et al.* (1973), which makes use of the  $R$  luminescence of a ruby chip placed in the cell. Their pressure sensor was calibrated with the use of fixed points at room temperature, which cannot be applied directly at low temperatures.

The  $R_1$  and  $R_2$  luminescence lines of ruby result from electronic transitions between the doublet state  ${}^2E$  and the  ${}^4A_2$  state of the chromium ion ( $Cr^{3+}$ ) in corundum ( $Al_2O_3$ ). The same lines, although not so wide, are found in the fluorescence spectrum of the sapphire windows of our cell which contain traces of chromium. At 4.2 K only the lower level of  ${}^2E$  is populated in the first step of de-excitation. Accordingly, only the  $R_1$  line is observed in the fluorescence spectrum and is quite sharp. The position,  $\sigma$ , of this  $R_1$  line was used as a pressure sensor after calibration by means of pressure runs employing solid helium to provide hydrostatic environment; with nitrogen, which is not plastic at this temperature one observes splitting of the  $R_1$  line (figure 1). The  $\sigma = f(p)$  curves obtained from different pressure cycles were reproducible to within  $\pm 60$  bars; correction for friction was made by averaging horizontally between the curves for increasing and decreasing pressure. The calibration curve (figure 2) was taken as the mean value of several experiments. The  $R_1$  line shift is not a linear function of the pressure, as found at normal temperatures for ruby by Barnett *et al.* (1973). The departure from linearity amounts to  $\sim \pm 150$  bars, which could be specific to low temperatures,

but could also be due to the complex strain conditions in the windows. The line shift is about  $0.84 \text{ cm}^{-1} \text{ kbar}^{-1}$  around 1 kbar, and  $0.6 \text{ cm}^{-1} \text{ kbar}^{-1}$  around 9 kbar, which is comparable to literature data for ruby. Thermal stabilisation of the windows is not a major problem, as the  $R$ -line temperature coefficient is quite negligible between 4 and 20 K. With account taken of the reproducibility of optical measurements and the inaccuracy associated with the calibration curve, the mean precision of pressure determination is  $\sim \pm 200$  bars.

In order to test the method, we have determined the  $\alpha$ - $\gamma$  transition pressure in solid nitrogen at 4.2 K. This phase transition can be detected from a simultaneous record of the low-frequency Raman spectra of both phases. The pressure is applied at  $\sim 70$  K when the solid is still plastic; and the cell is then cooled to 4.2 K. The pressure is determined at 4.2 K from the calibration curve. If the pressure is applied at 4.2 K, it is not hydrostatic, as seen from the Raman spectrum of  $\alpha$ - $N_2$  (figure 3): the lines are broadened, and the double degeneracy of the narrow  $E_g$  line is removed and the line is split. Thus under hydrostatic conditions, the  $\alpha$ - $\gamma$  transition occurs at  $\sim 3.65$  kbar (3600 atm). At 3.8 kbar the solid is entirely in its  $\gamma$  phase. According to Swenson (1955) this phase exists at low temperatures above 3500 atm. According to Schuch and Mills (1970) the  $\gamma$  transition at 19.5 K occurs at  $3945 \pm 70$  atm in  $^{28}N_2$  and 3535 atm in  $^{30}N_2$ .

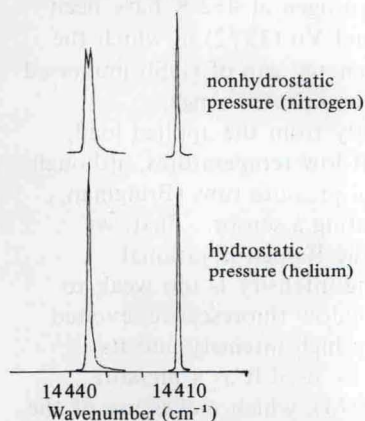


**Figure 1.** Profile of the fluorescence line of the sapphire window at 8.6 kbar with solid helium and solid nitrogen as the pressure-transmitting medium. The argon line was the reference line.

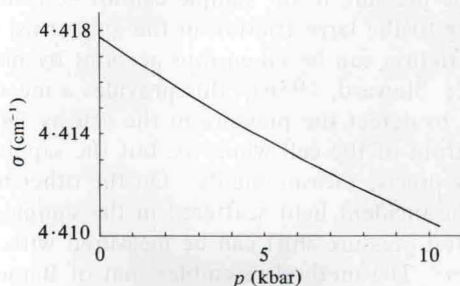


**Figure 2.** Calibration curve showing the wavenumber of the  $R_1$  fluorescence line of the cell sapphire windows,  $\sigma$ , as a function of pressure in the cell,  $p$ .

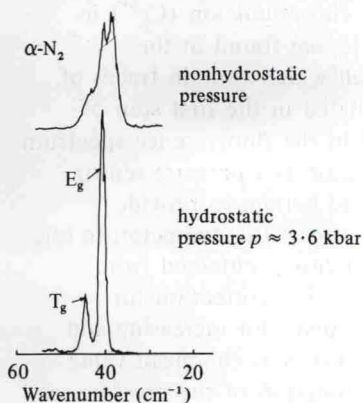


**Figure 3.** The effect of nonhydrostatic environment on the Raman spectrum of  $\alpha$ - $N_2$  at 7.2 K and 3.6 kbar.

### References

- Barnett, J. D., Block, S., Piermarini, G. J., 1973, *Rev. Sci. Instrum.*, **44**, 1-9.  
 Bridgman, P. W., 1942, *Proc. Am. Acad. Arts Sci.*, **74**, 425-440.  
 Fabre, D., Thiery, M. M., Vodar, B., 1975, *C. R. Acad. Sci. Ser. B*, **280**, 781.  
 Jean-Louis, M., Vu, H., 1972, *Rev. Phys. Appl.*, **7**, 89-94.  
 Schuch, A. F., Mills, R. L., 1970, *J. Chem. Phys.*, **52**, 6000-6008.  
 Stewart, J. W., 1956, *J. Phys. Chem. Solids*, **1**, 146-158.  
 Swenson, C. A., 1955, *J. Chem. Phys.*, **23**, 1963.

## Some important developments in the industrial application of the hydrostatic extrusion technology

J O H Nilsson

ASEA, Robertsfors, Sweden

The ASEA production presses have a maximum press force of 40 MN and are of the same basic Quintus<sup>®</sup> design for both cold and hot hydrostatic extrusion. Their main parts are the press frame and the container (figure 1). When load is applied during press operation, the columns become partly relieved but are still kept under compression even at the maximum press force. The container consists of a steel cylinder, which is prestressed by numerous layers of cold-rolled high-strength steel wire. The cylinder has a tapered bore in which a replaceable liner is inserted. This liner is so dimensioned that it acquires the desired tangential prestressing. The container is designed for an extrusion pressure up to 1400 MPa. High pressure seals are placed at the rear ends of the liner. The axial force on the seals by the high pressure fluid is balanced by four hydraulic rams. A floating piston is mounted in the liner bore. When fluid is pumped in, this piston is forced against the billet and firmly holds the billet and the die centred in the bore. The floating piston has relief valves which let fluid through to fill the space surrounding the billet.

A set of curves showing run-out extrusion pressure as a function of extrusion ratio for the cold hydrostatic extrusion of several materials is shown on figure 2. Aluminium and aluminium alloy allow extrusion ratios high enough for most practical applications. A billet for the extrusion of copper-clad aluminium consists of a core of aluminium enclosed in a copper tube. As the copper tube is usually thin-walled, the extrusion pressure is close to that for pure aluminium (figure 3). The copper tube and the aluminium billet are tapered at one end by milling, and annealed. They are then lined up and a pneumatic ram passes the aluminium bar into the copper tube. A steel plug is inserted into the rear end of the copper tube. The nose at the front of the copper tube is hydraulically upset in order to keep the loosely contained aluminium billet in position. The billet and die angles are chosen so that the pressure medium cannot escape in-between. Depending on the shape of the die orifice, rectangular sections (bus-bars) and round sections (wire) can be produced.

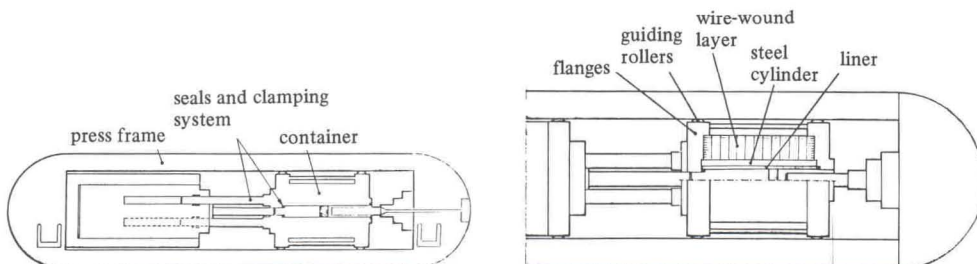


Figure 1. Cut-away views of the QUINTUS<sup>®</sup> hydrostatic extrusion press (left) and the container (right).

When busbars are extruded, they are cooled and guided through flying shears, which cut them into 20 m long lengths. They pass next to a straightening machine, after which they are cut into lengths and bundled. The extruded wire is guided through a cooling section and then up a guide tube in a loop and down into a steel drum, where it coils itself automatically. When the coiling has been completed, the steel drum and the coil are transferred to a joining station where the joining is accomplished by cold pressure welding. This station also contains a coiler for recoiling the joined wire into coils about 3 tons in weight.

The products produced have a high standard of surface finish and close tolerances. A fully satisfactory bond between copper and aluminium is obtained owing to the heavy deformation. Copper-clad aluminium has proved to be an excellent material for electrical conductors, combining the low price of aluminium and the good and reliable contact properties of copper.

For materials with higher resistance to deformation than aluminium and aluminium alloys, for instance copper and copper alloys, the extrusion ratio which is required for economical production of simple sections and tubes cannot be achieved with billets at room temperature. By increasing the billet temperature during extrusion to about 350°C the extrusion ratio is increased from 50 : 1 to about 1000 : 1 at 1400 MPa for copper, which is high enough for most practical applications (figure 4).

In the ASEA system for hot hydrostatic extrusion the pressure medium is charged into the container at low temperature and under comparatively high pressure (this permits the use of the pressure medium above its normal boiling temperature); only the billet and the die are preheated; and the quantity of pressure medium heated by the billet is kept to a minimum.

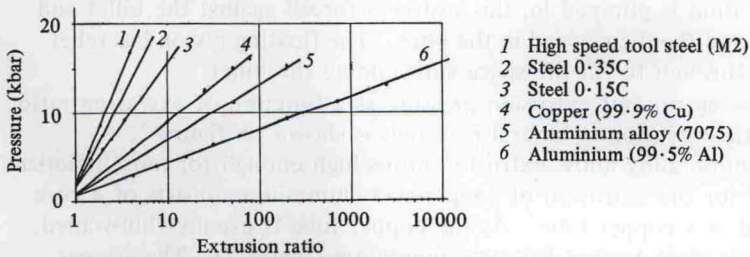


Figure 2. Pressure versus extrusion ratio for some common materials.

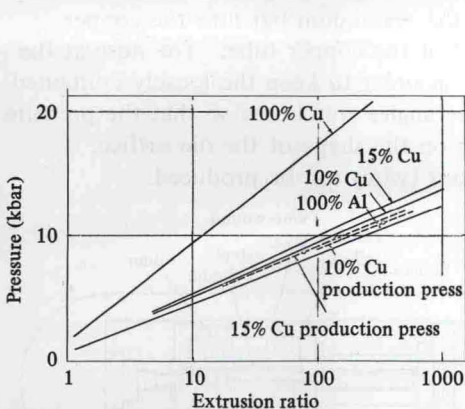


Figure 3. Extrusion pressure versus extrusion ratio for copper-clad aluminium with 100 mm billets (solid lines) and 170 mm billets (dashed lines). The percentages shown relate to the cross-section area.

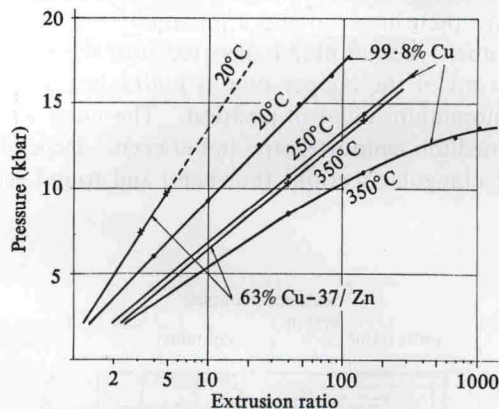


Figure 4. Extrusion pressure versus extrusion ratio for copper and brass at different temperatures.

---

**References**

- Barnett, J. D., Bean, V. E., Hall, H. T., 1966, *J. Appl. Phys.*, **37**, 875.  
Epain, R., Susse, C., Vodar, B., 1967, *C. R. Acad. Sci., Ser. A*, **265**, 323-326.  
Hall, H. T., 1960, "High pressure methods" in *International Symposium on High Temperature Technology*, Stanford Research Institute, Ed. C. A. Scarlott (McGraw-Hill, New York).  
Kawai, N., Mochizuki, S., Fujita, H., 1971, *Phys. Lett. A*, **34**, (2), 107.  
Kumazawa, M., 1971, *High Temp. - High Pressures*, **3**, 243-260.
- 

**Pressure determination in a high-pressure cell for Raman spectroscopy at 4.2 K****D Fabre**

Laboratoire des Interactions Moléculaires et des Hautes Pressions, CNRS, 92190 Meudon-Bellevue, France

When using Raman spectroscopy for investigating molecular interactions under pressure it is necessary to know the density or the pressure, neither of which can be readily determined in low-temperature experiments. The high-pressure Raman cell used here is of a piston-cylinder type (Jean-Louis and Vu, 1972) with four sapphire windows. It is not suited to density measurements, largely because of the presence of windows. Infrared absorption studies of hydrogen at 4.2 K have been made up to 14 kbar with such a device by Jean-Louis and Vu (1972) in which the pressure was determined from the pressure shift of the energy gap of GaSb immersed in the sample, but this method can be applied only in the infrared range.

The pressure in the sample cannot be estimated directly from the applied load, owing to the large friction in the apparatus, especially at low temperatures, although the friction can be taken into account by making several pressure runs (Bridgman, 1942; Steward, 1956); this provides a means of calibrating a sensor. First, we tried to detect the pressure in the cell by its effect on the Raman librational spectrum of the cell windows, but the sapphire scattering intensity is too weak to allow precise measurements. On the other hand, the window fluorescence, excited by the incident light scattered in the sample, has a fairly high intensity and its spectral pressure shift can be measured with precision; we used it as a pressure sensor. The method resembles that of Barnett *et al.* (1973), which makes use of the  $R$  luminescence of a ruby chip placed in the cell. Their pressure sensor was calibrated with the use of fixed points at room temperature, which cannot be applied directly at low temperatures.

The  $R_1$  and  $R_2$  luminescence lines of ruby result from electronic transitions between the doublet state  ${}^2E$  and the  ${}^4A_2$  state of the chromium ion ( $Cr^{3+}$ ) in corundum ( $Al_2O_3$ ). The same lines, although not so wide, are found in the fluorescence spectrum of the sapphire windows of our cell which contain traces of chromium. At 4.2 K only the lower level of  ${}^2E$  is populated in the first step of de-excitation. Accordingly, only the  $R_1$  line is observed in the fluorescence spectrum and is quite sharp. The position,  $\sigma$ , of this  $R_1$  line was used as a pressure sensor after calibration by means of pressure runs employing solid helium to provide hydrostatic environment; with nitrogen, which is not plastic at this temperature one observes splitting of the  $R_1$  line (figure 1). The  $\sigma = f(p)$  curves obtained from different pressure cycles were reproducible to within  $\pm 60$  bars; correction for friction was made by averaging horizontally between the curves for increasing and decreasing pressure. The calibration curve (figure 2) was taken as the mean value of several experiments. The  $R_1$  line shift is not a linear function of the pressure, as found at normal temperatures for ruby by Barnett *et al.* (1973). The departure from linearity amounts to  $\sim \pm 150$  bars, which could be specific to low temperatures,

but could also be due to the complex strain conditions in the windows. The line shift is about  $0.84 \text{ cm}^{-1} \text{ kbar}^{-1}$  around 1 kbar, and  $0.6 \text{ cm}^{-1} \text{ kbar}^{-1}$  around 9 kbar, which is comparable to literature data for ruby. Thermal stabilisation of the windows is not a major problem, as the *R*-line temperature coefficient is quite negligible between 4 and 20 K. With account taken of the reproducibility of optical measurements and the inaccuracy associated with the calibration curve, the mean precision of pressure determination is  $\sim \pm 200$  bars.

In order to test the method, we have determined the  $\alpha$ - $\gamma$  transition pressure in solid nitrogen at 4.2 K. This phase transition can be detected from a simultaneous record of the low-frequency Raman spectra of both phases. The pressure is applied at  $\sim 70$  K when the solid is still plastic; and the cell is then cooled to 4.2 K. The pressure is determined at 4.2 K from the calibration curve. If the pressure is applied at 4.2 K, it is not hydrostatic, as seen from the Raman spectrum of  $\alpha$ - $\text{N}_2$  (figure 3): the lines are broadened, and the double degeneracy of the narrow  $E_g$  line is removed and the line is split. Thus under hydrostatic conditions, the  $\alpha$ - $\gamma$  transition occurs at  $\sim 3.65$  kbar (3600 atm). At 3.8 kbar the solid is entirely in its  $\gamma$  phase. According to Swenson (1955) this phase exists at low temperatures above 3500 atm. According to Schuch and Mills (1970) the  $\gamma$  transition at 19.5 K occurs at  $3945 \pm 70$  atm in  $^{28}\text{N}_2$  and 3535 atm in  $^{30}\text{N}_2$ .

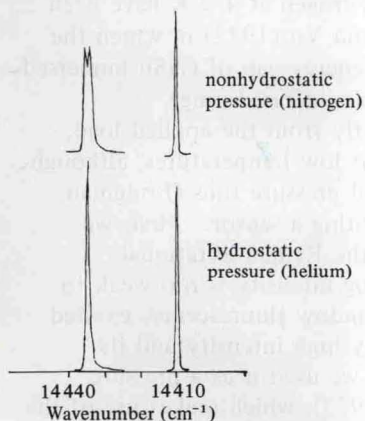


**Figure 1.** Profile of the fluorescence line of the sapphire window at 8.6 kbar with solid helium and solid nitrogen as the pressure-transmitting medium. The argon line was the reference line.

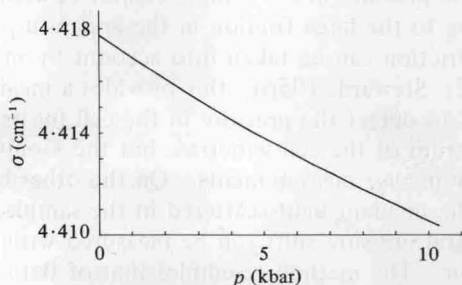


**Figure 2.** Calibration curve showing the wavenumber of the  $R_1$  fluorescence line of the cell sapphire windows,  $\sigma$ , as a function of pressure in the cell,  $p$ .

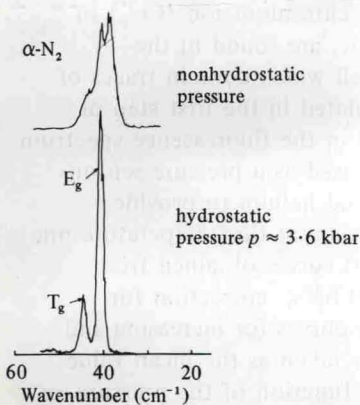


**Figure 3.** The effect of nonhydrostatic environment on the Raman spectrum of  $\alpha$ - $\text{N}_2$  at 7.2 K and 3.6 kbar.